Chapter 5

Effect of overexpression of *E. coli* NADH insensitive Y145F *cs* gene on production of organic acid in *B. japonicum* USDA110 and *M. loti* MAFF030669

5.1 INTRODUCTION

Citrate synthase (CS) is a ubiquitous enzyme that catalyzes the first committed step of tricarboxylic acid (TCA) cycle involving condensation of oxaloacetate (OAA) and acetyl-CoA to form citrate. Hence it is the key enzyme governing the carbon flux into the TCA cycle which plays a dual function in the production of cellular energy and biosynthetic precursors under aerobic conditions and only latter under anaerobic conditions, respectively (Park et al., 1994).

5.1.1 CS and NADH sensitivity

E. coli CS and the CS from other Gram-negative bacteria are allosteric enzymes was recognized almost 50 years ago. The CS of Gram-negative bacteria differ from those of Gram-positive bacteria and eukaryotes in that they are subjected to allosteric inhibition by NADH. NADH inhibition of *E. coli* CS is weakened by conditions, such as high salt or alkaline pH, which favor activity (Weitzman, 1966; Weitzman and Danson, 1976). Gram negative bacteria produce a 'large' homo-hexamer of identical subunits with monomer size of ~48kDa, contains 427 amino acid encoded by *gltA* gene, and is strongly and allosterically inhibited by NADH and, in the facultative anaerobes such as *E. coli,* also by 2-oxoglutarate (Weitzman 1981; Nguyen et al., 2001). On the other hand, gram-positive bacteria and all eukaryotes produce a 'small' (dimeric) also known as type I CS which is insensitive to NADH.

Pseudomonas CS is also allosteric and its kinetic properties suggest as an intermediate between *E. coli* and *Acinetobacter anitratum* enzymes (Massarini et al., 1975; Higa et al., 1978). Two forms of CS (EC 4.1.3.7) have been found in several species of *Pseudomonas,* a large form (Mr ~ 1: 250000) which is generally inhibited by NADH and a small form (Mr ~ 1: 100000) which is insensitive to these nucleotide effectors. Hence, the NADH sensitivity of gram negative bacterial CS is attributed to subunit size. A mutant of *Pseudomonas aeruginosa* PAC514 has been found to contain both a large (CSI) and a small (CSII) isozyme (Solomon and Weitzman, 1983; Mitchell

et al., 1995). The CS of gram-negative bacteria is an allosteric enzyme designated as type II. *E. coli* and *.A. anitratum* CS are strongly homologous in amino acid sequence and more distantly resemble the non-allosteric Type I CS of eukaryotes (Bhayana et al., 1984; Donald et al., 1987; Francois et al., 2006).

5.1.2: NADH insensitive CS

The distinctness of the NADH binding sites from the active sites is established by structural studies on a CS-NADH complex. *E. coli* CS exists in two conformational states, one of which (the R state) binds acetyl-CoA selectively, whereas the other (the T state) binds NADH selectively. NADH inhibition is competitive with respect to acetyl-CoA and noncompetitive with respect to the other substrate, OAA (Wright and Sanwal, 1971). NADH binding is competitively inhibited by acetyl-CoA (Duckworth and Tong 1976).

Type I dimers were altered by a series of mutations to generate NADH sites. Site-directed mutagenesis was used to prepare variant CS proteins in which the nine putative hydrogen-bonding residues in the NADH site, identified through the structural studies, were replaced by nonbonding residues (Maurus et al ., 2003). In addition, one particularly intriguing variant has been crystallized in the presence and absence of NADH, and the three-dimensional structures have been determined using x-ray diffraction methods (Duckworth et al., 2003.). The structure of the CS-NADH complex allows the prediction of a number of hydrogen bonds between NADH and the protein, including nine involving amino acid side chains. These variants are listed in **Table 5.1**, along with the effects of the amino acid substitutions on NADH binding and inhibition. Each variant protein was active and appeared to be stable. These three variants, Y145F, R163L, and K167A, all involve residues that are believed to take part in a complex hydrogen bonding network with the pyrophosphate moiety of NADH (**Fig.5.1**). All of the variants show some changes in NADH binding and inhibition and small but significant changes in kinetic parameters for catalysis. In three cases, Y145F, R163L, and K167A, NADH inhibition has become extremely weak.

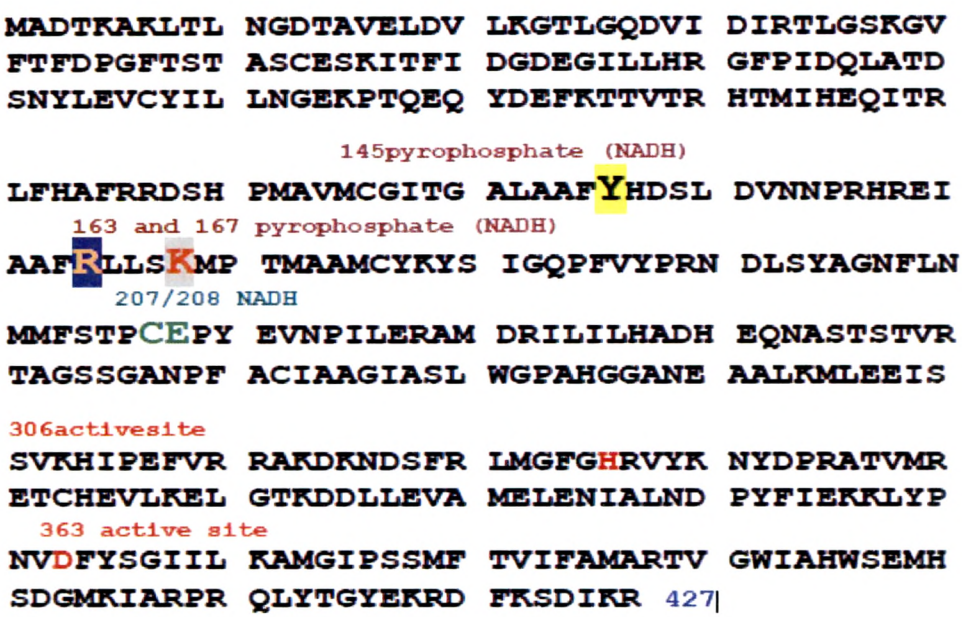

Fig. 5.1: *E. coli* CS protein sequence showing the regulatory variant (Duckworth et al., 2003.).

Table 5.1: NADH binding and inhibition by variant CSs (Stokell et al., 2003)

Variant	Kd (μM)	Ki (μM)	Maximum inhibition(%)
Wild type	1.6±0.1	2.8±0.4	100±10
R109L	1.16±.04	1.7±0.2	96±6
H110A	5.2±0.2	121±11	97±3
T111A	6.6±0.2	80±15	87±6
Y145F	>100	790±210	100±3
R163L	5.81±.04	400±80	77±8
K167A	4.1±0.2	630±130	100±10
Q128A	6.1±0.5	18±3	100±7
N189A	6.9±0.8	242±26	96±5
T204A	10.2±0.4	165±36	100±7

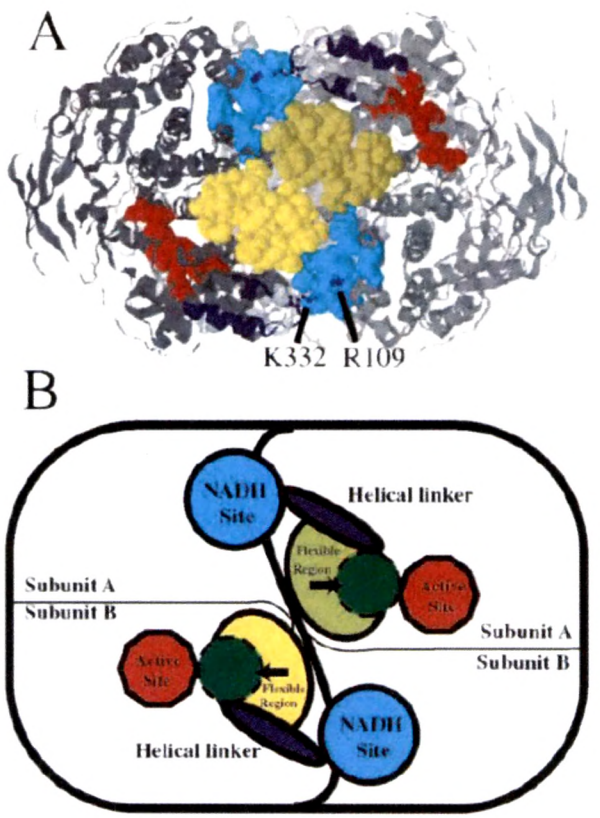

Fig. 5.2: **Route of communication between NADH binding sites and active sites in wild type hexameric *E. coli* CS** (Stokell et al., 2003).

Examination of the hexameric structure of *E. coli* CS as a whole showed that the helical linker region (residues 316–342) structurally links the refolded active site region polypeptide chain segment (residues 262–298) to an NADH binding site. However, the NADH binding site involved is not from the same subunit, instead being located across the dimer-dimer interface on an adjacent subunit (**Fig. 5.2. A and B)** (Stokell et al., 2003).

5.1.3: Increase in production of Citric acid

Isocitrate lyase (*icl*) gene overexpression in *Yarrowia lipolytica* altered citrate/isocitrate ratio towards citric acid (Forster et al., 2007a). Additionally, invertase gene expression enabled *Y. lipolytica* to secrete high levels of citric acid in presence of sucrose. Similarly, *B. subtilis* mutant in early stationary phase accumulated ~15 fold higher intracellular citrate levels as compared to the wild type (Matsuno et al., 1999). Metabolic studies on citric acid producing fungi, yeasts, and *E. coli* demonstrated that high citric acid levels could be attained on glucose and depending on the host metabolism. Disruption of *icd* gene of *E. coli* has been reported to secrete citric acid levels up to 3.4 mM (Aoshima et al., 2003; Kabir and Shimizu, 2004). Although citric acid was increased, the mutant showed glutamate auxotrophy. However, citric acid secretion is difficult to explain as *E. coli* K strain does not possess citrate transporter (Hall, 1982). Citric acid secretion was also found in *Bacillus subtilis icd* and *Streptomyces coelicolor* aconitase mutants (Matsuno et al., 1999; Viollier et al., 2001).

Increase in CS activity was postulated to be a better strategy for citric acid production in *E. coli* rather than isocitrate dehydrogenase (*icd*) mutation which reduces biomass and growth (Aoshima et al., 2003). Overexpression of *E. coli cs* gene in *Pseudomonas fluorescens* ATCC 13525 yielded millimolar levels of intracellular and extracellular citric acid (Buch et al., 2009). The amount of citric acid produced by *P. fluorescens* overexpressing *E. coli cs* gene was similar to that secreted by the phosphate solubilizing *Bacillus coagulans* and *Citrobacter koseri* on glucose but the levels were insufficient for releasing P from soils (Gyaneshwar et al., 1998; Srivastava et al., 2006).

Metabolic studies in *E. coli* demonstrated that high citric acid yields could be attained on glucose and depending on the host metabolism; glucose transport, flux though catabolic pathways and the regulatory mechanisms influenced by intracellular metabolite pools appear to facilitate the citrate accumulation (Elias, 2009). To increase the flux through the anaplerotic node for increasing oxaloacetate levels, *ppc* gene of *S. elongatus* was over-expressed in *P. fluorescens* 13525. *ppc* gene overexpression enhanced cellular biomass, glucose catabolism through intracellular phosphorylative pathway and resulted

in increased gluconic, pyruvic and acetic acids and intracellular citric acid but citric acid was not secreted. Overexpression of either of *ppc* and *cs* genes enhanced MPS ability of *P. fluorescens* 13525 on Pikovskya's agar; but *ppc-cs* co-expression neither altered *P. fluorescens* ATCC 13525 metabolism nor affected the citrate production (Buch et al., 2010). Overexpression of *E. coli* CS *gltA* gene in *Pseudomonas fluorescens* ATCC 13525 yielded intracellular and extracellular citric acid levels during the stationary phase, respectively (Buch et al., 2009). Hence further strategies are required to increase the citrate level.

Among the three CS variants studied, Y145F showed maximum inhibition, highest Ki and Kd values (Stokell et al., 2003) Also *Pf* (pY145F) showed the highest CS activity amongst all the other variants which is 2 fold,1.7 fold and 1.96 fold higher as compared to the wild type *cs* bearing strain *Pf* (pAB7) and other two NADH insensitive *cs* bearing strain *Pf* (pR163L) and *Pf* (K167A) respectively in the mid log phase, so pY145F was used for further study (Adhikary, 2012).

Partial sequencing of pY145F plasmid

Partial sequencing of the PCR product amplified from pY145F plasmid when analysed using NCBI BLAST (Basic Local Alignment Search Tool) and Ribososmal Database Project (RDP) II, online homology search programs, revealed maximum identity (99%) to *E. coli* CS (GenBank Accession number AAA23892) (**Fig. 5.3 and 5.4**).

>YFPCRPRODUCT_YFFOR_S702

CNCNNANCGGCACCCTGAACGGGGATACAGCTGTTGAACTGGATGTGCTGAA
AGGCACGC TGGGTCAAGATGTTATTGATATCCGTACTCTCGGTTCAAAAGGT
GTGTTCACCTTTGACCCAGGCTTCACTTCAACCGCATCCTGCGAATCTAAAAT
TACTTTTATTGATGGTGATGAAGGTATTTTGCTGCACCGCGGTTTCCCGATCG
ATCAGCTGGCGACCGATTCTAACTACCTGGAAGTTTGTTACATCCTGCTGAAT
GGTGAAAAACCGACTCAGGAACAGTATGACGAATTTAAAACTACGGTGACCC
GTCATACCATGATCCACGAGCAGATTACCCGTCTGTTCCATGCTTTCCGTCGC
GACTCGCATCCAATGGCAGTCATGTGTGGTATTACCGGCGCGCTGGCGGCGT
TCTTTCACGACTCGCTGGATGTTAACAATCCTCGTCACCGTGAAATTGCCGCG
TTCCGCCTGCTGTCGAAAATGCCGACCATGGCCGCGATGTGTTACAAGTATTC
CATTGGTCAGCCATTTGTTTACCAGCGCAACGATCTCTCCTACGCCGGTAACT
TCCTGAATATGATGTTCTCCACGCCGTGCGAACCGTATGAAGTTAATCCGATT
CTGGAACGTGCTATGGACCGTATTCTGATCCTGCACGCTGACCATGAACAGA
ACGCCTCTACCTCCACCGTGCGTACCGCTGGCTCTTCGGGTGCGAACCCGTTT
GCCTGTATCGCAGCAGGTATTGCTTCACTGTGGGGACCTGCGCACGGCGGTG
CTAACGAAGCGGCGCTGAAAATGCTGGAAGAAATCAGCTCCGTTAAACACA
TTCCGGAATTTGTTCGTCGTGCGAAAGACAAAAATGATTCTTTCCGCCTGATG
GGCTTCGGTCACCGCGTGTACAAAATTACGACCCGCGCGCCACCGTAATGCG
TGAAACCTGCCATGAAGTGCTGAAAGAGCTGGGCACGAANNTGACCTGCTGN
AGT

Fig. 5.3: Partial sequence of *E. coli* NADH insensitive *cs* gene.

>gb|U00096.2| Escherichia coli str. K-12 substr. MG1655, complete genome
Length=4639675

Features in this part of subject sequence:
citrate synthase

Score = 1777 bits (962), Expect = 0.0
Identities = 971/975 (99%), Gaps = 1/975 (0%)
Strand=Plus/Minus

Query	4	CACCCTGAACGGGGATACAGCTGTTGAACTGGATGTGCTGAAAGGCACGCTGGGTCAAGA	63
Sbjct	753668	CACCCTCAACGGGGATACAGCTGTTGAACTGGATGTGCTGAAAGGCACGCTGGGTCAAGA	753609
Query	64	TGTTATTGATATCCGTACTCTCGGTTCAAAAGGTGTGTTCACCTTTGACCCAGGCTTCAC	123
Sbjct	753608	TGTTATTGATATCCGTACTCTCGGTTCAAAAGGTGTGTTCACCTTTGACCCAGGCTTCAC	753549
Query	124	TTCAACCGCATCCTGCGAATCTAAAATTACTTTTATTGATGGTGATGAAGGTATTTTGCT	183
Sbjct	753548	TTCAACCGCATCCTGCGAATCTAAAATTACTTTTATTGATGGTGATGAAGGTATTTTGCT	753489
Query	184	GCACCGCGGTTTCCCGATCGATCAGCTGGCGACCGATTCTAACTACCTGGAAGTTTGTTA	243
Sbjct	753488	GCACCGCGGTTTCCCGATCGATCAGCTGGCGACCGATTCTAACTACCTGGAAGTTTGTTA	753429
Query	244	CATCCTGCTGAATGGTGAAAAACCGACTCAGGAACAGTATGACGAATTTAAAACTACGGT	303
Sbjct	753428	CATCCTGCTGAATGGTGAAAAACCGACTCAGGAACAGTATGACGAATTTAAAACTACGGT	753369
Query	304	GACCCGTCATACCATGATCCACGAGCAGATTACCCGTCTGTTCCATGCTTTCCGTCGCGA	363
Sbjct	753368	GACCCGTCATACCATGATCCACGAGCAGATTACCCGTCTGTTCCATGCTTTCCGTCGCGA	753309
Query	364	CTCGCATCCAATGGCAGTCATGTGTGGTATTACCGGCGCGCTGGCGGCGTTCTTTCACGA	423
Sbjct	753308	CTCGCATCCAATGGCAGTCATGTGTGGTATTACCGGCGCGCTGGCGGCGTTCTATCACGA	753249
Query	424	CTCGCTGGATGTTAACAATCCTCGTCACCGTGAAATTGCCGCGTTCCGCCTGCTGTCGAA	483
Sbjct	753248	CTCGCTGGATGTTAACAATCCTCGTCACCGTGAAATTGCCGCGTTCCGCCTGCTGTCGAA	753189
Query	484	AATGCCGACCATGGCCGCGATGTGTTACAAGTATTCCATTGGTCAGCCATTTGTTTACCA	543
Sbjct	753188	AATGCCGACCATGGCCGCGATGTGTTACAAGTATTCCATTGGTCAGCCATTTGTTTACCC	753129
Query	544	GCGCAACGATCTCTCCTACGCCGGTAACTTCCTGAATATGATGTTCTCCACGCCGTGCGA	603
Sbjct	753128	GCGCAACGATCTCTCCTACGCCGGTAACTTCCTGAATATGATGTTCTCCACGCCGTGCGA	753069
Query	604	ACCGTATGAAGTTAATCCGATTCTGGAACGTGCTATGGACCGTATTCTGATCCTGCACGC	663
Sbjct	753068	ACCGTATGAAGTTAATCCGATTCTGGAACGTGCTATGGACCGTATTCTGATCCTGCACGC	753009

Fig. 5.4: NCBI BLAST analysis of partial *cs* sequence.

Pair wise alignment of the sequence with original *E. coli* K12 NADH sensitive *cs* sequence from database using EBI pair wise alignment tool, revealed a mutation of tyrosine residues in 146 amino acid position to phenylalanine (**Fig. 5.5**).

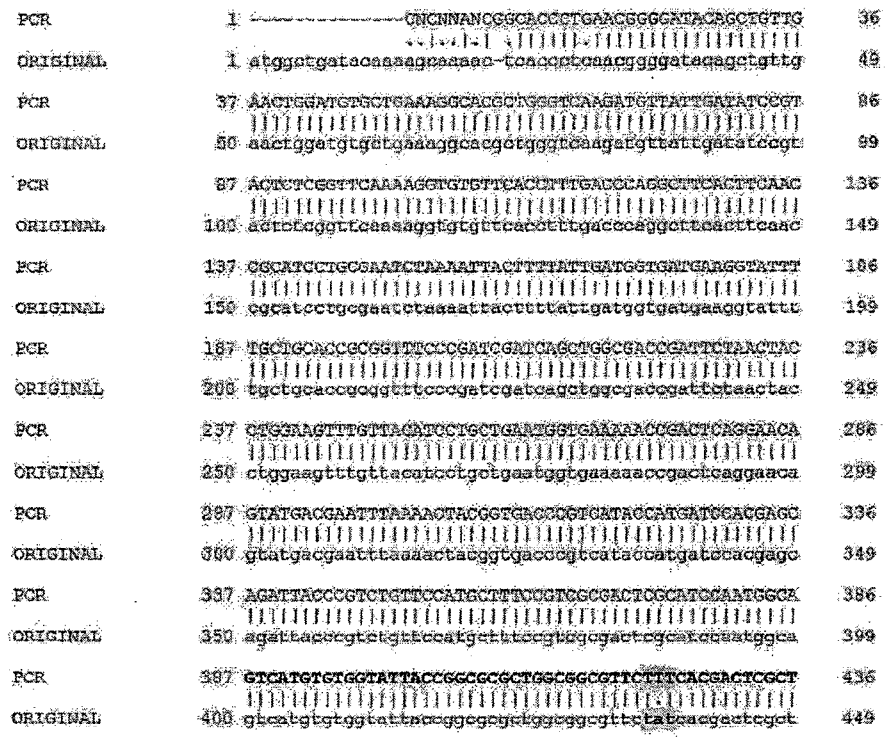

Fig. 5.5: EBI pair wise alignment of NADH insensitive and wild type *cs* gene showing the position of mutation.

To increase the flux through the anaplerotic node for increasing oxaloacetate levels, NADH insensitive *cs* gene was over-expressed in fluorescent *P. fluorescens* PfO-1 which resulted in significant increase in CS activity and citric acid levels as compared to the wild type NADH sensitive CS *P. fluorescens* PfO-1 harboring pY145F showed maximum CS activity of 333.4±8.5U on M9 minimal medium in the presence of 100 mM glucose which is ~ 5.6 fold higher than that in the control *Pf* (pAB8) (Adhikary, 2012). The NADH insensitive *cs* gene overexpression caused significant alterations in both intracellular and extracellular citric acid levels and yields. Intracellular citric acid levels in *Pf* (pY145F) increased by 5.7, 6.9 and 2.6 fold while there is a 5, 7.9 and 2.9 fold increase in intracellular citrate yield as compared to wild type strain, *Pf* (pAB8)and *Pf* (pAB7), respectively. Corresponding extracellular citrate levels increased by 57, 51.6 and

1.9 fold with an increase of extracellular citrate yield by 39.8, 29.9 and 2.39 fold compared to respective controls (**Fig. 5.6;** Adhikary et al., 2012).

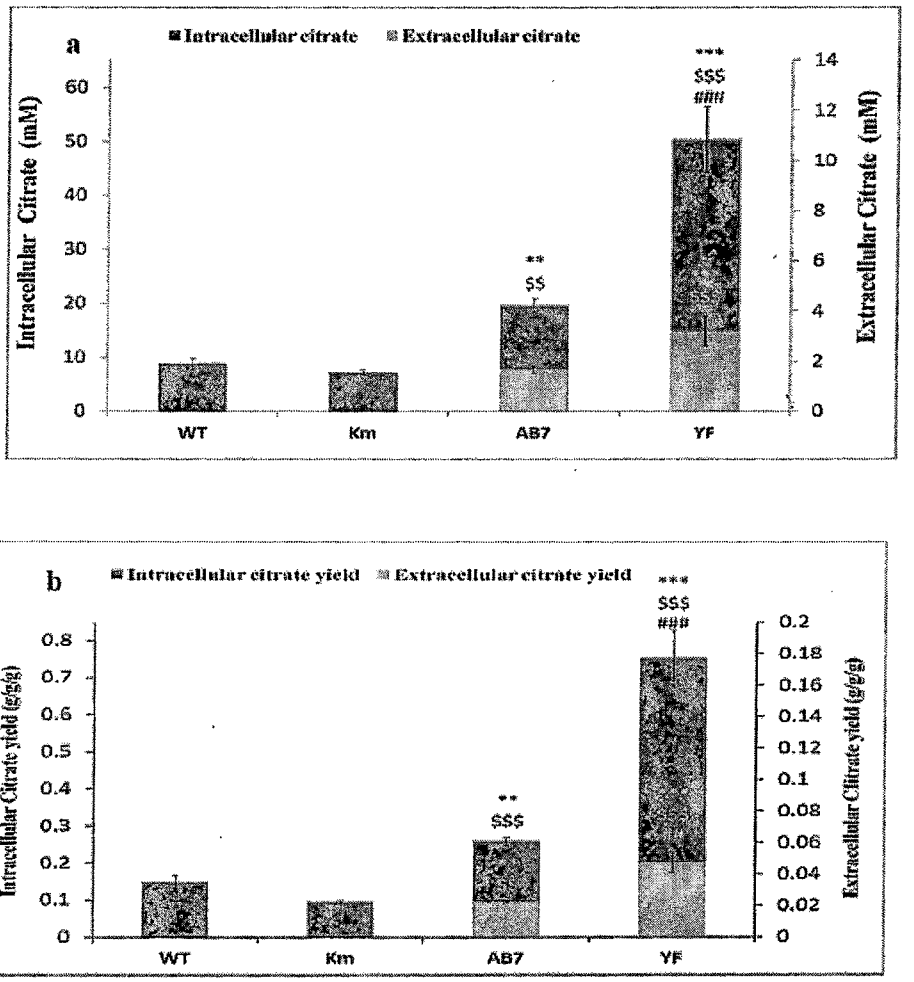

Fig. 5.6: Citric acid levels and yields in *P. fluorescens* PfO-1 wild type and plasmid bearing strains Km, AB7 and YF. Intracellular citrate levels (a) and yields (b) are represented in black bars and extracellular citrate levels (a) and yields (b) are represented in grey bars.

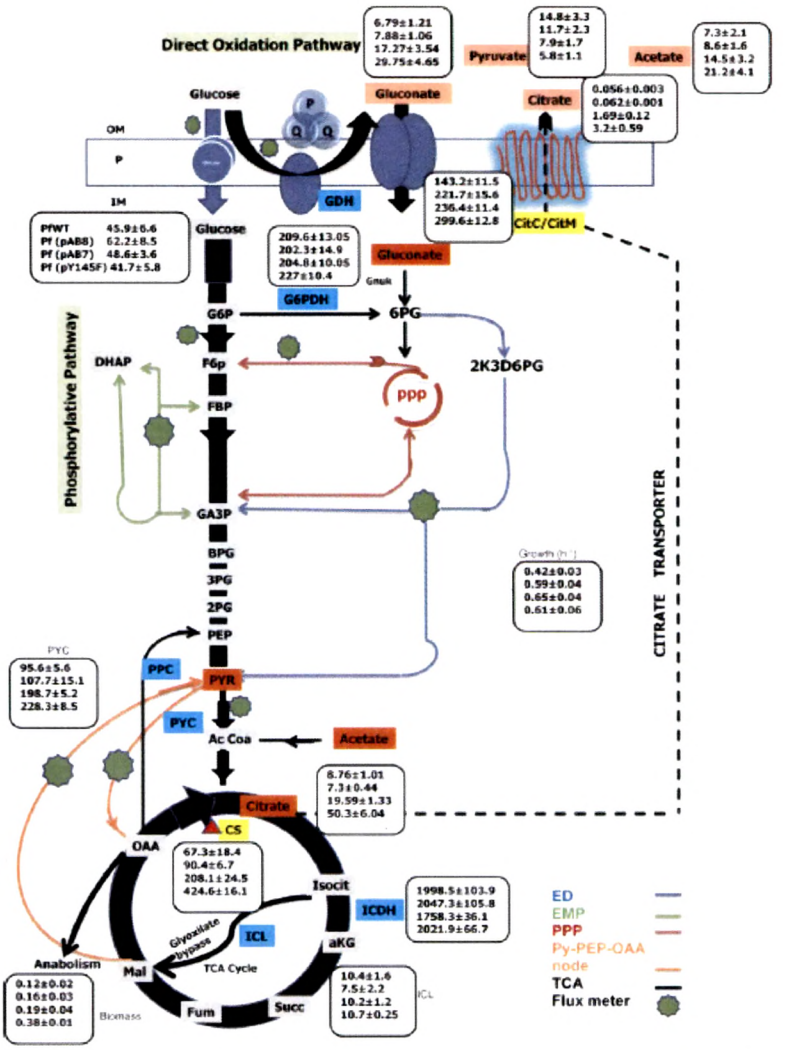

Fig. 5.7: Key metabolic fluctuations in *P. fluorescens* PfO-1 overexpressing NADH insensitive *E. coli* CS.

5.1.4 Rational of the present study

Overexpression of *ppc* gene of *S. elongatus* in *B. japonicum USDA110* and *M. loti MAFF030669* enhanced cellular biomass, glucose catabolism through intracellular phosphorylative pathway and resulted in increased gluconic and citric acids secretion, this high citric acid was due to increased activities of both PYC and PPC. Similarly,

overexpression of *gltA* gene of *E. coli* in the last chapter also resulted in significant increase in citric acid secretion upto 7 mM due to significant increase in the activity of CS. However, P solubilization was better in *ppc* gene overexpression as compared to *glt* gene overexpression which could be attributed to the lower levels of gluconic acid in the latter case. In order to further increase citric acid secretion, this chapter dealt with developing *Rhizobium* strains expressing *E. coli* NADH insensitive *cs* gene and monitoring its effects on citric acid accumulation and secretion and glucose metabolism.

5.2: Experimental design

The experimental plan of work includes the following-

5.2.1: List of bacterial strains used

All wild type and genetically modified *E. coli* and *Rhizobium* strains used in this study are listed in **Table 2.1 and 2.2**. The plasmids used in the present study and their restriction maps are given in **Table 2.3** and **Fig. 2.1**. *E. coli* JM101 was used for all the standard molecular biology experiments wherever required

Table 5.2 list of bacterial strains

Bacterial strains	Characteristics	Source/Reference
	***E. coli* strains**	
E. coli JM101	Used for molecular biology experiments	Sambrook and Russell, 2001
E. coli W620	*cs* mutant strain exhibiting glutamate auxotrophy, CGSC 4278 - *glnV44 gltA6 galK30 LAM-pyrD36 relA1 rpsL129 thi-1*; Str^r	*E. coli* Genetic Stock Center
S 17.1 (pAB7) *E. coli*	*S 17.1* with pAB7 plasmid; Amp^r, Km^r	Buch et al, 2008
S 17.1 (pAB8) *E. coli*	*S 17.1* with pAB8 plasmid; Amp^r, Km^r	Buch et al, 2008
	***Rhizobium* strains**	
Bradyrhizobium japonicum USDA110	NC_004463.1	NCBI
Mesorhizobium loti	NC_002678.2	NCBI

MAFF030669		
Bj (pJNK3)	*B. japonicum* USDA110 with pJNK3 plasmid; Ap^r, Km^r (*E. coli* NADH insensitive *cs*)	This study
Bj (pAB8)	*B. japonicum* USDA110 with pAB8 plasmid; Ap^r, Km^r (control vector)	This study
Ml (pJNK3)	*M. loti* MAFF030669 with pJNK3 plasmid; Ap^r, Km^r (*E. coli* NADH insensitive *cs*)	This study
Ml (pAB8)	*M. loti* MAFF030669 with pAB8 plasmid; Ap^r, Km^r (control vector)	This study

5.2.2: Details of Plasmid used

pUCPM18 with *E. coli* NADH insensitive *cs** gene under *Plac* , Ap^r and km^r gene, named as pJNK3 was used in this chapter.

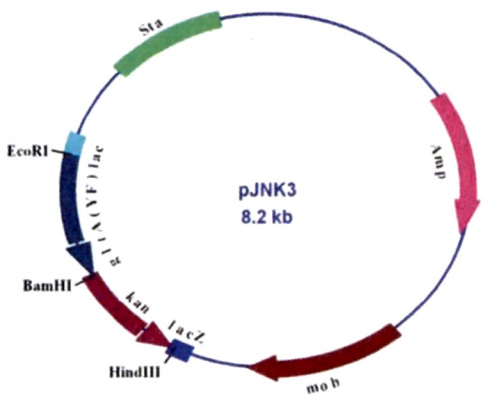

Fig. 5.8: Restriction map of the plasmid used in this chapter (Wagh et al., 2013).

5.3: RESULTS

5.3.1: Heterologous overexpression of *E. coli* NADH insensitive *cs** gene in *Rhizobium* spp.

The plasmids incorporated in *B. japonicum* USDA110 and *M. loti* MAFF030669 transformants were isolated from the transformants and were confirmed based on restriction digestion pattern before studying the effect of overexpression of *E. coli* NADH insensitive *cs** gene (**Fig. 5.9**).

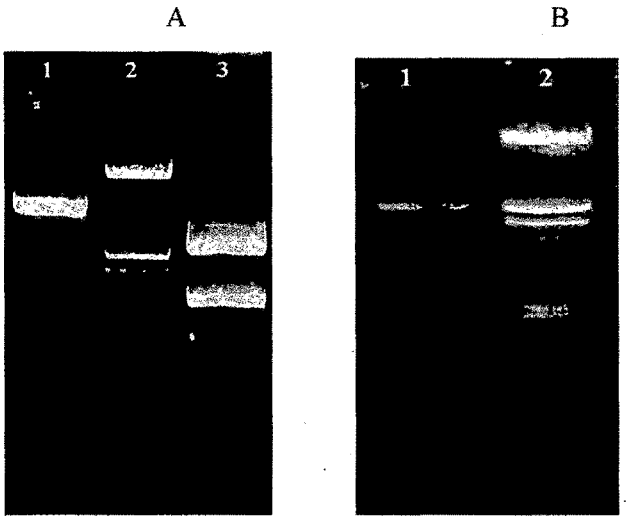

Fig. 5.9 : Restriction Digestion pattern of plasmids containing pJNK3 isolated from transformants of (A) *B. japonicum* USDA110 and (B) *M. loti* MAFF030669 Lane 1: pJNK3 linear with HindIII (8.26 kbp); Lane 2: Molecular Weight Marker (MWM)-Lambda DNA cut with ECORV/ HIND III; Lane 3: pJNK3 digested with EcoRI-HindIII (5,298bp, 2,967bp); Lane 1: pJNK3 digested with EcoRI-HindIII (5,298bp, 2,967bp); Lane 2: Molecular Weight Marker (MWM)-Lambda DNA cut with EcoRV/ Hind III.

The CS activity estimated in *B. japonicum* USDA110 and *M. loti* MAFF030669. harboring *E. coli* NADH insensitive *cs* gene {*Bj* (pJNK3)} and{ *Ml* (pJNK3)} grown on TRP medium with 50mM glucose, was 3.4 and 4.8 fold higher (62.41 ±.0.48 U and 67.02

± 1.98 U) in both the strains compared to control which possessed very low levels of CS activity (18.64 ± 1.26 U) and (13.89 ± 0.83 U).

To check MPS ability a zone of clearance and acidification was observed on PVK and TRP plates respectively and the maximum zone of clearance and acidification was shown by *Bj* (pJNK3) and *Ml* (pJNK3) as compared to the control *Bj* (pAB8) and *Ml* (pAB8).P-solubilizing ability of wild type *B. japonicum* USDA110 and *M. loti* MAFF030669 and its transformants varied in the order of *Bj* (p JNK3) = *Ml* (p JNK3) > *Bj* (pAB8) = *Ml* (pAB8) >*Bj*=*Ml* on PVK medium after 3 days of incubation at 30°C (**Fig. 5.10**).

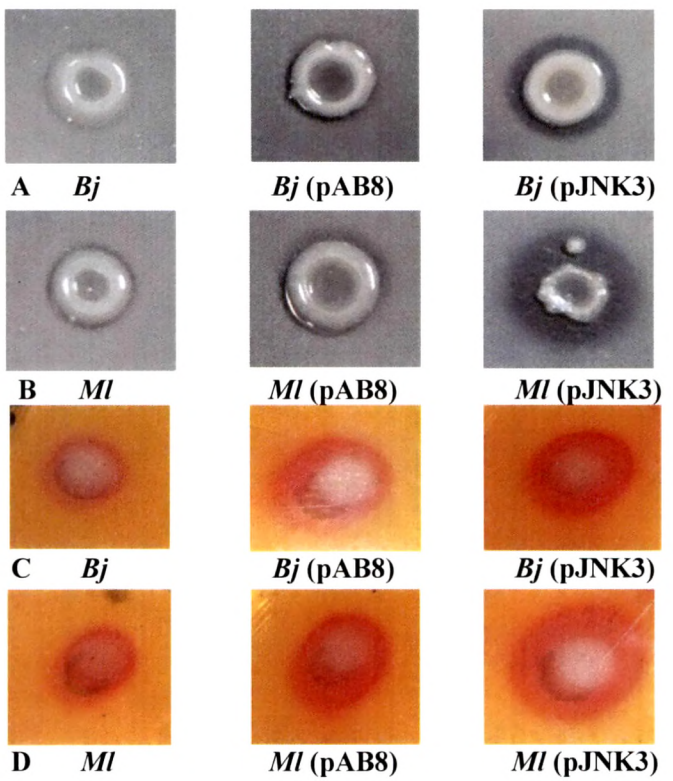

Fig. 5.10: MPS phenotype of *B.japonicum* USDA110(a), (c) and *M. loti* MAFF030669 (b),(d) harboring pJNK3 plasmid expressing *cs* gene. Zone of clearance formed by *Rhizobium* transformants on Pikovskaya's agar and Tris rock phosphate agar containing

50mM glucose The results were noted after an incubation of 3days at 30 °C. Media composition and other experimental details are as described in Sections 2.2.4 and 2.7.

Table 5.3: P solubilization index on Pikovskyas agar of *B.japonicum* USDA110 and *M. loti* MAFF030669 transformants during 3 days of growth *Bj* and *Ml*: wild type strain; Bj (pAB8): *B.japonicum* with vector control and *Bj* (pJNK3) : *B.japonicum* with NADH insensitive *cs* gene. The results were noted after an incubation of 3 days at 30 °C and are given as mean ± S.D. of three independent observations as compared to native *Bj and Ml.*

***Rhizobium* Strains**	**Diameter of zone of clearance (mm)**	**Diameter of colony (mm)**	**Phosphate Solubilizing Index**
Bj	12.17 ± 0.29	11.17 ± 0.29	1.09
***Bj* (pAB8)**	11.17 ± 0.29	9.50 ± 0.50	1.22
***Bj* (pJNK3)**	14.50 ± 0.50	10.17 ± 0.29	1.44
Ml	12.83 ± 0.29	11.50 ± 0.50	1.09
***Ml* (pAB8)**	12.17 ± 0.29	10.17 ± 0.29	1.22
***Ml* (pJNK3)**	16.83 ± 0.29	10.17 ± 0.29	1.60

The pJNK3 transformants of *B. japonicum* USDA110 and *M. loti* MAFF030669 showed maximum enhanced zone of clearance as compared to the control pAB8. Phosphate Solubilizing Index was calculated as described in 2. And it was highest in *Bj* (pJNK3) and *Ml* (pJNK3) **(Table 5.3).**

5.3.5: Effect of *E. coli* NADH insensitive *cs* gene overexpression on growth pattern and pH profile in presence of 50mM glucose concentrations.

The growth profiles and organic acid secretion of *Bj* (pAB8) , *Bj* (pJNK3), *Ml* (pJNK3) and *Ml* (pAB8) along with native, on TRP medium with 50 mM glucose demonstrated that maximum O.D. was reached faster in transformants (12h compared to 20h of the control *Bj* (pAB8) and *Ml* (pAB8). Acid production was monitored and it was

found that there was slight pH drop within 20 h in the native and control vector while pH drop to 4.3 and 4.2 was seen in *Bj* (pJNK3) and *Ml* (pJNK3). Significant media acidification was seen within 12 h in both the cases. Both *Bj* (pJNK3) and *Ml* (pJNK3) acidified the medium when grown on TRP medium **(Fig. 5.11).**

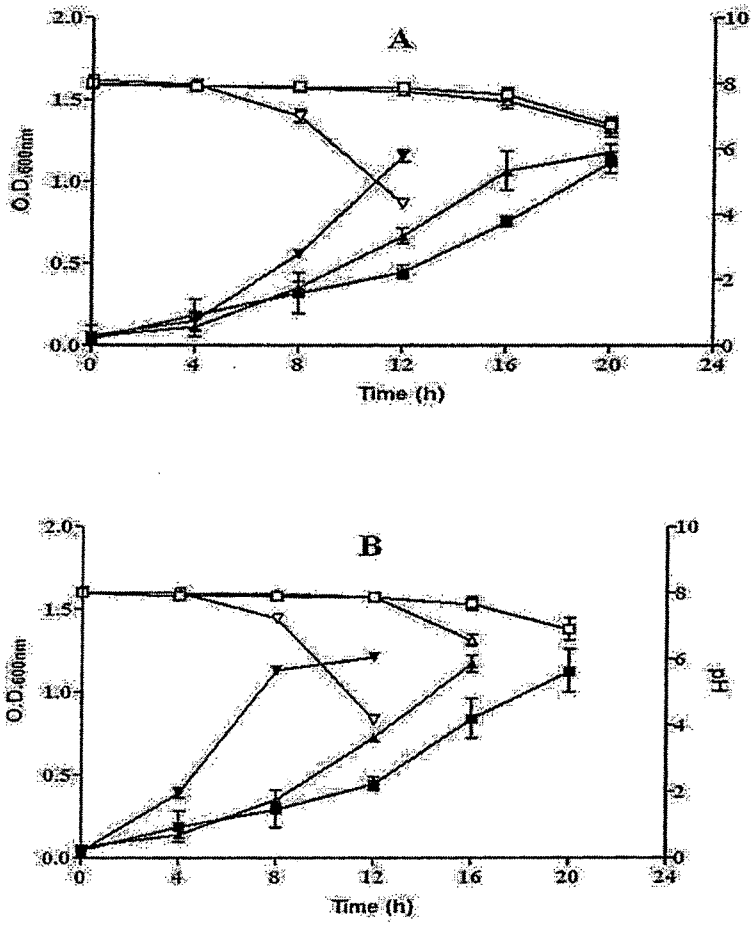

Fig. 5.11: Effect of *E. coli* NADH insensitive *cs* gene overexpression on extracellular pH (□, Δ, ▽,) and growth profile (■, ▲, ▼) of (A) *B. japonicum* USDA110 and (B) *M. loti* MAFF030669, on TRP medium with 50 mM glucose .(□, ■, *Bj, Ml* wild type); {Δ, ▲, *Bj* (pAB8), *Ml* (pAB8)}; {▽, ▼, *Bj* (pJNK3), *Ml* (pJNK3)}. OD_{600} and pH values at each time point are represented as the mean ± SD of six independent observations.

5.3.7: Physiological effects of *E. coli* NADH insensitive *cs* gene overexpression on TRP medium with 50 mM glucose.

In presence of 50 mM glucose, increase in CS activity significantly affected growth profile in transformants of both the strains (**Fig. 5.11**). The total glucose utilization rate showed negligible increase and the total amount of glucose consumed showed ~1.9 fold and ~1.8 fold decrease in *Bj* (pJNK3) and *Ml* (pJNK3) respectively at the time of pH drop. The increase in CS activity increased biomass yield by ~1.6 fold and also ~1.7 fold decrease was seen in specific glucose utilization rate in the transformants of both the *Rhizobium* strains (**Table 5.4**).

Table 5.4: Physiological variables and metabolic data from of *B. japonicum* USDA110 and *M. loti* MAFF030669 *cs transformants grown on TRP medium.** The results are expressed as Mean ± S.E.M of 6 independent observations. *a* Biomass yield $Y_{dcw/Glc}$, specific growth rate (k) and specific glucose utilization rate (Q_{Glc}) were determined from mid log phase of each experiment. *b* Total glucose utilized and glucose consumed were determined at the time of pH drop. The difference between total glucose utilized and glucose consumed is as explained in Section 2.9.3. *** P<0.001.

Rhizobium Strains	Specific Growth Rate $k(h^{-1})^a$	Total Glucose Utilized (mM) ^{b}	Glucose Consumed (mM) ^{b}	Biomass Yield $Y_{dcw/Glc}$ (g/g) ^{a}	Specific Glucose Utilization Rate Q_{Glc} $(g.g\ dcw^{-1}.h^{-1})^a$
Bj	0.186±0.03	46.20 ±0.2	38.23±1.33	1.78 ±0.14	0.14 ±0.01
***Bj* (pAB8)**	0.229±0.02	46.01 ±0.31	37.11±0.33	1.57 ±0.29	0.17 ±0.04
***Bj* (pJNK3)**	0.259±0.01	48.07 ±0.10	19.61±0.48***	2.54 ±0.11***	0.10 ±0.01***
Ml	0.221±0.03	45.91 ±0.64	37.07±0.55	1.36 ±0.26	0.19 ±0.04
***Ml* (pAB8)**	0.258±0.02	46.01 ±0.51	37.07±0.71	1.06 ±0.07	0.24 ±0.02
***Ml* (pJNK3)**	0.381±0.03	48.15 ±0.30	20.91±1.50***	1.73 ±0.09***	0.14 ±0.01***

5.3.6: Biofilm, exopolysaccharide and indole acetic acid production by *Bj* (pJNK3) and *Ml* (pJNK3) transformants in TRP medium.

Biofilm showed significant increase by ~2.2 and ~2.75 fold in *Bj* (pJNK3) and *Ml* (pJNK3) respectively, compared to control, exopolysaccharide production was increased by ~1.6 fold in both the transformants compared to control vectors. Indole acetic acid production was increased by ~1.5 fold in *Bj* (pJNK3) and ~1.3 fold in *Ml* (pJNK3). This increase helped in phosphorus release by overexpression of *cs* gene when grown in TRP medium 100mM Tris-Cl Buffer pH 8 and 50mM Glucose containing Rock Phosphate 1mg/ml in comparison to control (**Table 5.5**).

Table 5.5: Biofilm, exopolysaccharide and indole acetic acid production by *Bj* (pJNK3) and *Ml* (pJNK3) transformants in TRP medium.The results are expressed as Mean ± S.E.M of 6-10 independent observations *** P<0.001.

Rhizobium Strains	Biofilm O.D.at 550nm	EPS (g/100ml)	IAA (µg/ml)
Bj	1.96 ±0.03	12.48 ±0.24	20.14 ±1.33
Bj (pAB8)	2.08 ±0.03	13.41 ±0.63	25.54 ±0.81
Bj (pJNK3)	4.53 ±0.22***	21.95 ±0.71***	38.03 ±1.06***
Ml	1.51 ±0.06	13.55 ±2.78	30.16 ±2.34
Ml (pAB8)	1.54 ±0.06	15.65 ±0.51	26.65 ±2.18
Ml (pJNK3)	4.24 ±0.1***	24.31 ± 1.83***	34.66 ±0.55***

5.3.5: P Solubilization and Organic acid secretion by *Bj* (pJNK3) and *Ml* (pJNK3) transformants in TRP medium.

There was significant increase in release of P by ~13 fold in both the transformants compared to control vectors when grown in TRP medium containing 50 mM glucose (**Fig. 5.12**).

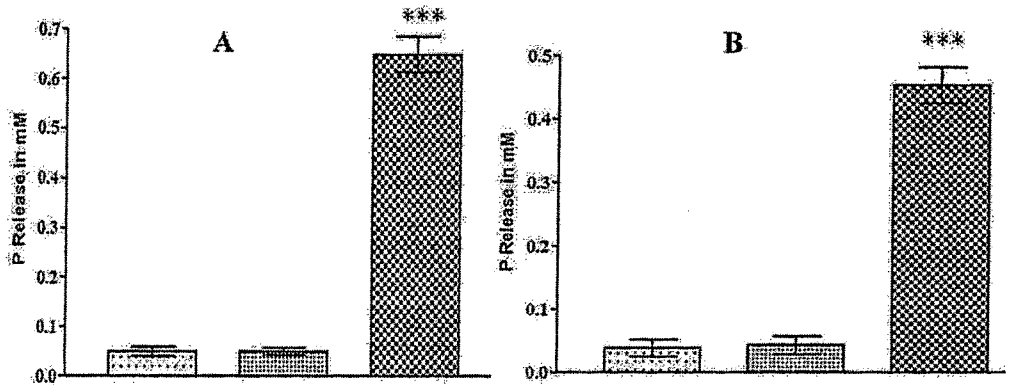

Fig. 5.12: P solubilization by (A) *B. japonicum* USDA110 , (B) *M. loti* MAFF030669 transformants on TRP medium. (▭, *Bj*, *Ml* wild type); {▭, *Bj* (pAB8), *Ml* (pAB8)}; {▭, *Bj* (pJNK3), *Ml* (pJNK3)}; the values are depicted as Mean ± S.E.M of 7-10 independent observations. *** P<0.001.

On TRP medium in presence of 50 mM glucose, the organic acids identified were mainly gluconic, 2-ketogluconic, acetic and citric acids. As a result of *E. coli* NADH insensitive *cs* gene overexpression, there was only quantitative change in two organic acids secreted. Due to overexpression of *cs** gene, there was ~10.8 and~11.1 fold increase in citric acid with their corresponding increase in yield ($Y_{C/G}$) by ~5.7 and ~4.9 fold in *B. japonicum* USDA110 and *M. loti* MAFF030669 *E. coli* NADH insensitive *cs* gene transformants, respectively. Also extracellular medium of *Bj* (pJNK3) and *Ml* (pJNK3) contained ~4 and ~3.7 fold higher amount of gluconic acid, and~2.3 and~1.8 fold increase in its yield was seen respectively as compared to *Bj* (pAB8) and *Ml* (pAB8) **(Fig. 5.13)**.Intracellular citric acid levels remained unchanged **(Table 5.6).**

Table 5.6: Intracellular citric acid production by *Bj* (pJNK3) and *Ml* (pJNK3) transformants in TRP medium.

Rhizobium Strains	Intracellular Citric acid in mM	*Rhizobium* Strains	Intracellular Citric acid in mM
***B.japonicum* USDA110**	0.83 ± 0.06	***M. loti* MAFF030669**	0.85 ± 0.04
***Bj* (pAB8)**	0.75 ± 0.05	***Ml* (pAB8)**	1.15 ± 0.06
***Bj* (pJNK3)**	0.73 ± 0.06	***Ml* (pJNK3)**	0.81 ± 0.03

Results are expressed as Mean ± S.E.M of 4-6 independent observations. * P<0.05, ** P<0.01 and *** P<0.001.

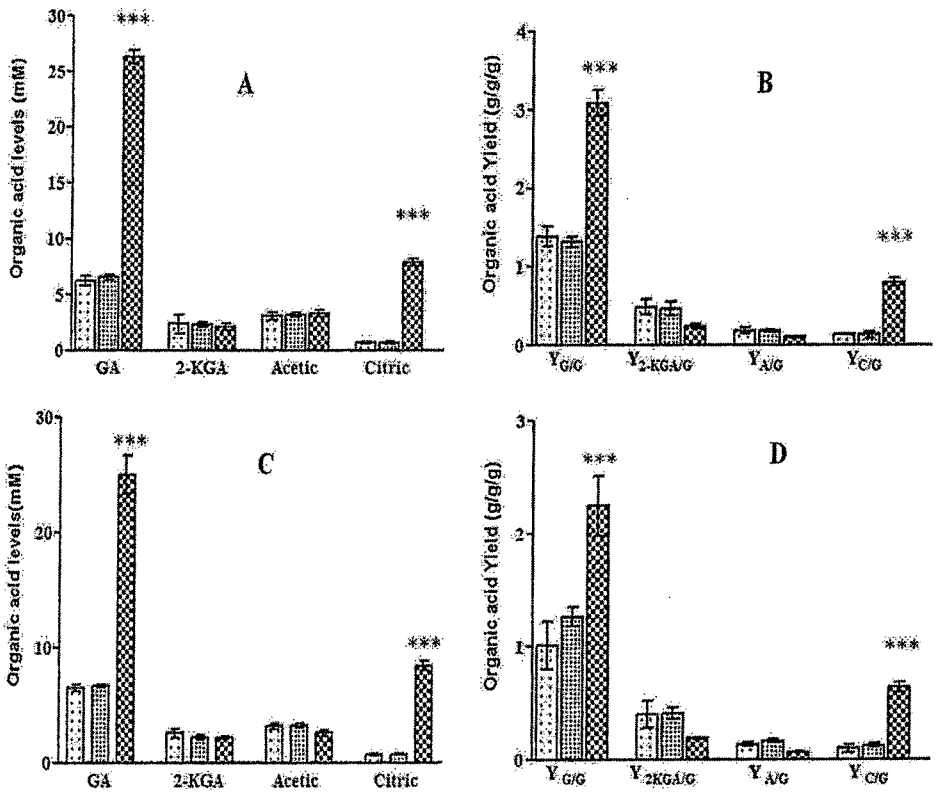

Fig. 5.13: Organic acid production {(a) and (c)} and Yield {(b) and (d)} from *B. japonicum* USDA110 *and M. loti* MAFF030669 *cs* gene transformants, respectively. All organic acids are estimated from stationary phase cultures (at the time of pH drop) grown on TRP medium with 50mM glucose. Results are expressed as Mean ± S.E.M of 4-6 independent observations *** P<0.001.**(ii) Alterations in enzyme activities in *Bj* (pAB3) and *Ml* (pJNK3)**

In order to correlate the alterations in physiological variables and organic acid profile, enzymes involved periplasmic direct oxidation and intracellular phosphorylative were estimated. In response to *cs** gene overexpression, about ~ 3.4 and ~ 4.8 fold increase is seen in CS activity in *Bj* (pJNK3) and *Ml* (pJNK3), respectively. GDH activity increased by about ~1.5 and ~1.3 fold, respectively, as compared to the control, PYC showed ~2.3 and ~3.2 fold increase, respectively, in the transformants. The activity of G-6-PDH showed ~1.5 and ~1.4 fold increase in the transformants and also there was ~1.5 and ~1.9 fold increase in ICDH activity. The activity of PPC in *Bj* (pJNK3) and *Ml* (pJNK3) did not alter significantly as compared to the control. Glyoxylate pathway enzyme ICL also remained unaltered in *Bj* (pJNK3) and *Ml* (pJNK3) (**Fig. 5.14**).

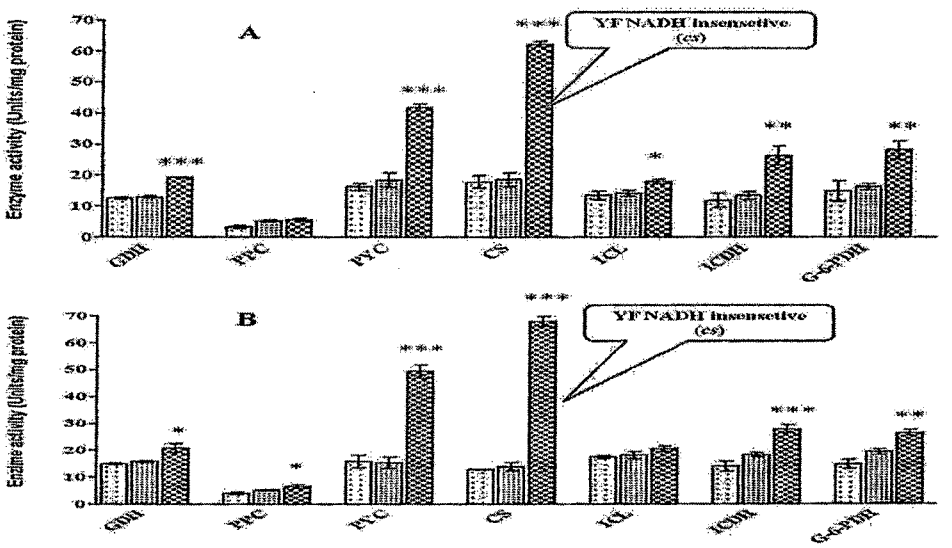

Fig. 5.14: Activities of enzymes PPC, PYC, GDH, G-6-PDH, ICDH and ICL in *B. japonicum* USDA110 and *M. loti* MAFF030669 *ppc* transformants. The activities have been estimated using cultures grown on TRP medium with 50mM glucose. All the enzyme activities were estimated from mid log phase to late log phase cultures except CS, ICDH and ICL which were estimated in stationary phase (Section 2.10). All the enzyme activities are represented in the units of nmoles/min/mg total protein. The values are depicted as Mean±S.E.M of 7-10 independent observations. * P<0.05, ** P<0.01and *** P<0.001.

5.4: DISCUSSION

Present study demonstrates the effect of overexpression of NADH insensitive *E. coli cs* gene in *B. japonicum* USDA110 and *M. loti* MAFF030669. CS activity showed ~3.4 fold and ~4.8 fold increase in *Bj* (pJNK3) and *Ml* (pJNK3), respectively, as compared to the control and 1.1 and ~1.6 fold increase compared to the strain bearing the wild type *cs* gene. In earlier work when NADH insensitive *E. coli cs* was constitutively overexpressed under *lac* promoter in *Pf* O1 a maximum of 5.6 fold and 2 fold overexpression was obtained in *Pf* (Y145F) as compared to the control and strain bearing the wild type *cs* gene (Adhikary., 2012). In other earlier work when *E. coli* wild type *cs* gene was constitutively overexpressed under *lac* promoter in *P. fluorescens* ATCC 13525, 2 fold enhanced activity was observed compared to the control strain (Buch et al., 2009).

In the present study, as a consequence of increase in CS activity in *Bj* (pJNK3) and *Ml* (pJNK3) there is a ~11 fold elevated extracellular citrate level in both and ~5.7 and 4.9 fold increase, respectively in the yield .But there is no change in the intracellular levels of citrate. While an increase of ~6.9 fold and ~2 fold in intracellular citrate and ~51.6 fold increase and ~26 fold increase in extracellular citrate was seen in *Pf* O1 overexpressing NADH insensitive *E. coli cs* gene and *P. fluorescens* ATCC13525 overexpressing *E. coli* wild type *cs* gene, respectively (Buch et al 2009; Adhikary 2012). In another study *icd* mutant of *E. coli* K and B strains resulted in an increase of ~3.8 and 2.5 fold CS activities and enhanced citrate accumulation but unlike our study, in this case citrate accumulation had a negative effect on growth of the *E. coli* strains (Aoshima et al., 2003). Overexpression of mitochondrial CS genes also resulted in increased citrate efflux in cultured carrot cells (Koyama et al. 1999), *Arabidopsis* (Koyama et al. 2000), and canola plants (Anoop et al. 2003).

Increase in extracellular citrate levels by ~11 fold in both the strains compared to the control suggests an efficient flux system in *Rhizobium*, which is not seen in *P. fluorescens*. Increase in intracellular citrate level and yield by 1.9 and 2.39 fold, respectively, in *Pf* (pY145F) compared to *Pf* (pAB7) does not lead to similar increase in

extracellular citrate levels. Citric acid being the substrate of central carbon metabolism must be transported into and out of the cell for efficient bioactivity. Therefore low level of extracellular citrate can be attributed to weak efflux transport mechanism in *P. fluorescens* (Buch et al 2009; Adhikary, 2012).

Increased gluconic acid levels could be explained by increased PYC activity in *Bj* (pJNK3) and *Ml* (pJNK3), which could probably diverts pyruvate flux towards increased OAA biosynthesis to meet the increased CS activity. Even in *A. niger,* the enhancement of anaplerotic reactions replenishing TCA cycle intermediates predisposes the cells to form high amounts of citric acid (Legisa and Mattey, 2007). However, *cs* overexpression in *A. niger* did not affect PYC activity (Ruijter et al., 2000). Enhancement of biosynthetic reactions due to shortage of TCA cycle intermediates was also observed in citric acid accumulating *E. coli* K and B strains in the form of increased glyoxylate pathway (Aoshima et al., 2003; Kabir and Shimizu, 2004).

ICL activity remained unaltered in both the strains, which was similar to studies done in *Pf* O1 overexpressing NADH insensitive *E. coli cs* gene and *P. fluorescens* ATCC13525 overexpressing *E. coli* wild type *cs* gene, respectively (Buch et al 2009; Adhikary 2012). Low ICL activity was consistent with earlier reports in *P. fluorescens* ATCC13525 and *P. indigofera* in which ICL contributed negligibly to glucose metabolism (Buch et al., 2009; Diaz-Perez et al., 2007).

GDH and G-6-PDH activities increased by ~1.5 and ~1.3 fold in *Bj* (pJNK3) and *Ml* (pJNK3), respectively, suggesting an increase in periplasmic glucose oxidation and phosphorylative pathway. Enhanced CS activity in *Pf* (pY145F) also increased the periplasmic glucose oxidation which is reflected by increase in GDH activity and gluconic acid production. Moreover, significant decrease in glucose consumption without affecting the glucose utilization suggested the involvement of direct oxidation pathway for carbon flux distribution in *P. fluorescens.* The increased carbon flow through glycolysis led to increased protein synthesis that is reflected to increased biomass (Adhikary et al., 2012). The citrate induced oligosaccharide synthesis was reported in *Agrobacterium* sp. ATCC 31749 (Ruffing et al., 2011).

The central carbon metabolism network gets to the heterologous overexpression of NADH insensitive *E. coli cs* in *B. japonicum* USDA110 and *M. loti* MAFF030669 (**Fig. 5.15**). The conditions created in the present work include: improvement of glucose uptake, improvement of CS activity and citrate production compared to the earlier report by Buch et al. (2009) and Adhikary et al (2012) (**Fig. 5.16**). increased direct oxidation of glucose leading to more gluconate production and increased phosphorylative pathway.

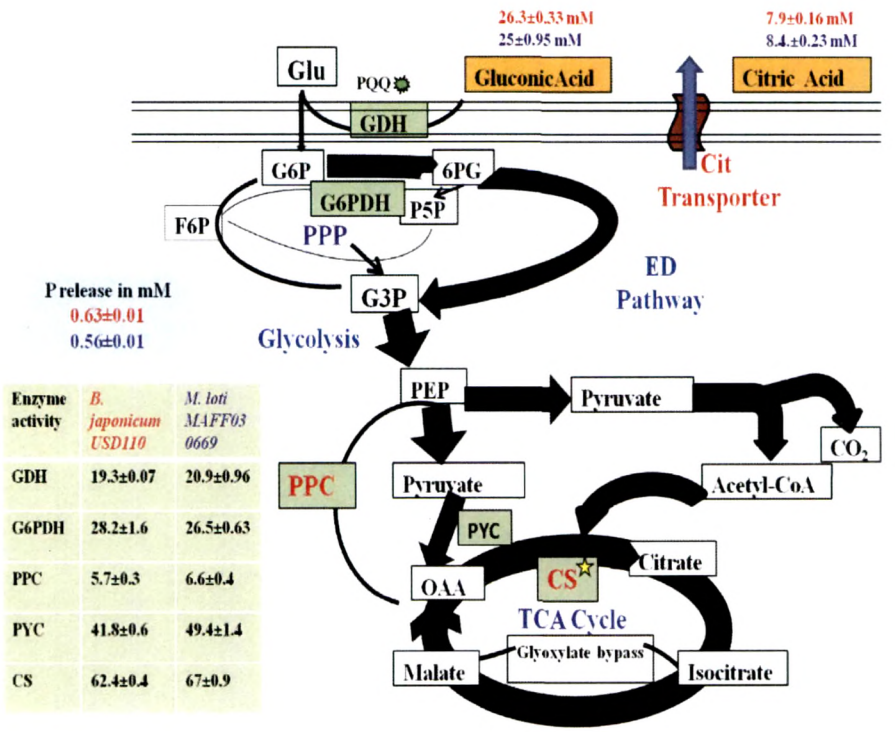

Enzyme activity	*B. japonicum USD110*	*M. loti MAFF030669*
GDH	19.3±0.07	20.9±0.96
G6PDH	28.2±1.6	26.5±0.63
PPC	5.7±0.3	6.6±0.4
PYC	41.8±0.6	49.4±1.4
CS	62.4±0.4	67±0.9

Fig. 5.15: Key metabolic fluctuations in *B. japonicum* USDA110 and *M. loti* MAFF030669 overexpressing NADH insensitive *E. coli cs* gene.

P solubilization was increased by *B. japonicum USDA110* and *M. loti MAFF030669* strains containing pJNK3 plasmids due to increase in the production of gluconic acid and citric acid. Similar observation is also reported in *Pf* (pAB7) and *Pf* O-1 (pY145F) as compared to their respective controls (**Fig. 5.16**) (Buch et al., 2010; Adhikary, 2012).

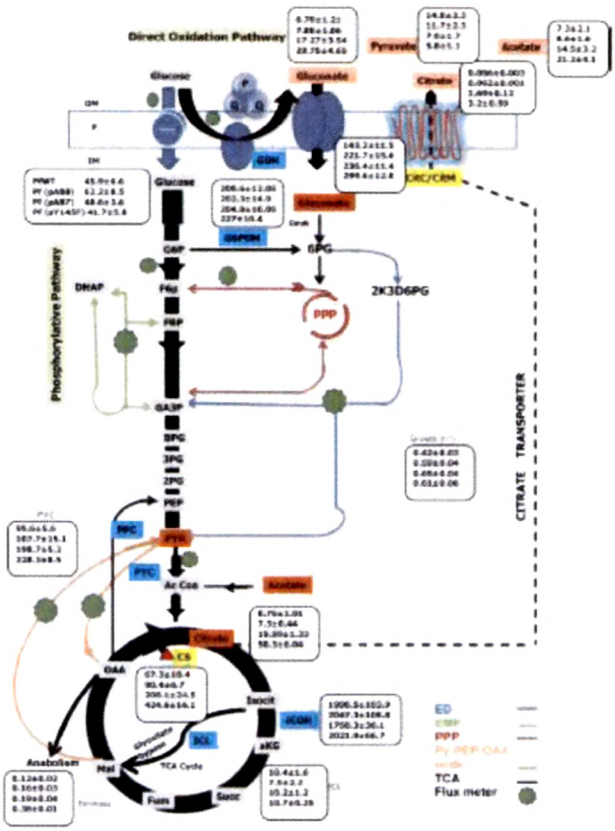

Fig. 5.16: Key metabolic fluctuations in *Pseudomonas* overexpressing NADH insensitive *E. coli cs* gene (Adhikary, 2012

P solubilization by *Rhizobium* transformants was better compared to overexpression of wild type *cs* gene due to increased amount of gluconic acid as well as citric acid levels.

Both *Rhizobium* transformants had enhanced growth promoting activities such as biofilm formation, exopolysaccharide and indole acetic acid production. It is not clear whether EPS synthesis in *Rhizobium* transformants is related to CS activity. Increase in biofilm formation and IAA production could be a consequence of improved metabolism in TRP medium.